Determination of Net Pay Cutoffs using Flow Simulation and Percolation Theory

Jason A. M^{c}Lennan[1], Thies Dose[2] and Clayton V. Deutsch[1]

[1]Centre for Computational Geostatistics (CCG) –Edmonton, Alberta
[2] RWE Dea Aktiengsellschaft – Hamburg, Germany

An important aspect of the evaluation of oil and gas reservoirs is the differentiation of reservoir and non-reservoir sections. This most frequently requires the application of net pay cutoff values on any kind of scale. These cutoff values are applied to the volume fraction of shale, porosity and perhaps permeability and water saturation at the reservoir evaluation stage. Many complicating factors influence the definition of net pay and the selection of appropriate net pay cutoffs. The nature of the geological heterogeneities and the recovery process are important aspects.

This paper introduces a framework for determination of reservoir-specific cutoff values within a consistent theoretical and practical framework. Flow simulation is applied on realistic small scale models of heterogeneity to establish the percolation threshold as a function of geological environment. Several reservoir-specific complexities are studied numerically and analytically within this framework. The methodology represents an integrated approach to net pay determination.

Introduction

Virtually all petroleum reservoir evaluations involve a determination of net pay. Net pay is the total reservoir material that will flow some economical amount of hydrocarbon under a particular production mechanism (Etris, 2004). The importance of net pay thickness is concerning hydrocarbon in place and reserve estimation if unquestioned (Dose, 2005). However, there is no set practice or methodology to separate net pay intervals from non-net pay intervals.

Leaving net pay determination to the flow simulator alone is dangerously optimistic. The notion that low permeability flow blocks will simply not permit flow in an economic amount of time is tempting. However, the requirement to upscale permeabilities to large scale flow blocks effectively masks significant non-net reservoir material. That is, a significant proportion of detailed non-net heterogeneity can be upscaled into recoverable flow. There is a need to apply net cutoff criteria at the reservoir evaluation stage for accurate recoverable reserve characterization.

The approach for determining net pay varies widely throughout the petroleum industry; however, it is always based on some sort of cutoff criteria. Although there is no fixed terminology, there are generally three net material classifications (Worthington, 2003), namely, net sand, net reservoir, and net pay. Figure 1 illustrates one application of petrophysical cutoff values to determine these net material classifications for a schematic gross reservoir interval. Net sand thickness is the total gross reservoir thickness that is not shale; net reservoir is all net sand material above a porosity and/or permeability threshold; and net pay is determined as the total net reservoir thickness that is above a water saturation cutoff. Figure 1 is a literary example; in practice, there is no set criterion.

Currently, the literature agrees that the determination of net pay depends on the specific reservoir under evaluation. For example, a simple reservoir volumetric evaluation may have different porosity and permeability cutoffs than the same reservoir being evaluated under a dynamic steam flood recovery mechanism. There have even been developments towards determining separate cutoff criteria for primary depletion and secondary waterflood depletion (Cobb, 1998). Unfortunately, documentation of these fit-for-purpose net pay cutoff criteria are mostly qualitative. There are still no quantitative or unambiguous methodologies for determining petrophysical property cutoff values. In particular, there are no relationships between net pay cutoff criteria and reservoir heterogeneity.

We propose a methodology for determining net pay petrophysical cutoff values tied back to theoretically determined net pay permeabilities. The net pay permeability cutoffs are determined using percolation theory; that is, the transition from net to non-net permeabilities is taken at the percolation threshold. The percolation threshold is a theoretical transition between net and non-net effective permeabilities and separates potential net or connected flow blocks from non-net or unconnected flow blocks. The values of the petrophysical at the percolation threshold can then be applied to log data to determine net pay intervals.

The overall steps of the methodology are: (1) construct a 3D geological model of lithofacies and petrophysical properties, (2) perform flow simulation for effective permeabilities, (3) plot effective permeability versus the petrophysical properties, (4) fit the effective permeability versus petrophysical property relationship to determine the percolation threshold, and (5) set the cutoff values equal to the petrophysical property value at the percolation threshold.

The percolation threshold values will change depending on several reservoir-specific parameters. The dependencies investigated in this work are (1) global shale proportion, (2) spatial shale correlation, (3) net to non-net permeability contrast, (4) the permeability distribution, (5) the geological to flow block size contrast, and (6) depositional setting. The aim of this work is to establish relationships between percolation threshold values and these reservoir heterogeneities.

The methodology can be fully automated so that the variation of net pay cutoffs according to several reservoir specific parameters such as global shale proportion, correlation structure, permeability distribution, modeling scale, and reservoir scale can easily be observed numerically. The cutoff criteria and their quantification are supported by theory, repeatable, and an unambiguous determination of net pay.

Using Percolation Theory for Net Pay Determination

Percolation theory in a petroleum context is referred to as correlated percolation, because the spatial distribution of the porous medium properties is correlated within a finite domain. Figure 2 illustrates correlated percolation for a small synthetic reservoir. The 2 x 2 array of squares in Figure 2(a) is a simple flow simulation grid. Figure 2(b) represents a geological block model indicating net (shaded) and non-net (unshaded) reservoir material. The net reservoir blocks that have a common side or corner constitute a connected path through which hydrocarbon can be recovered and are referred to as percolating clusters if they span the flow block in any direction. Five percolating clusters are outlined in Figure 2(b) with a broken line.

A pressure gradient is applied to the geological model (Figure 2(b)) and the steady-state flow rate and absolute effective permeability is calculated at each of the four flow simulation blocks. The recoverable flow rates are shaded in Figure 2(c). The volume fraction of shale V_{SHL} (proportion of white geological blocks) is also reported. Each of the three flow blocks yielding recoverable hydrocarbons contains a percolating cluster and relatively low V_{SHL} value. As V_{SHL} decreases, the possibility of forming a percolating cluster increases and eventually there is a critical V_{SHL} value ($V_{PT\text{-}SHL}$) where percolating clusters first begin to form. This critical threshold is of particular concern in petroleum applications and is called the percolation threshold.

The percolation threshold petrophysical properties can be theoretically determined for some simple configurations. For example, the critical threshold for random, isotropic shale in 3D is $V_{PT\text{-}SHL} = 0.69$ (Deutsch, 1989). In this work, the volume fraction of shale percolation threshold $V_{PT\text{-}SHL}$ will be determined numerically under several different reservoir heterogeneities for which there is no theoretical solution. A numerical procedure is developed and implemented for several reservoir-specific characteristics.

Figure 3 is a plot of absolute effective horizontal permeabilities versus volume fraction of shale V_{SHL} for an 8 x 8 x 4 block (Easting - *X*, Northing - *Y*, and Elevation - *Z* directions, respectively) flow simulation. The geological model is a synthetic 64 x 64 x 32 correlated sandstone/shale reservoir where each block is given a constant sand permeability and constant porosity of 1000mD and 0.40, respectively, or a shale permeability and porosity of 0.001mD and 0, respectively. As the volume fraction of shale increases, the effective permeability decreases. However, there is a clear transition between net permeabilities and non-net permeabilities at a V_{SHL} value of 70%. This $V_{PT\text{-}SHL}$ value is the largest fraction of shale to allow a connected path through which hydrocarbons can flow and be recovered economically. This value is called the percolation threshold and the corresponding V_{SHL} value is referred to as the percolation threshold volume fraction of shale or $V_{PT\text{-}SHL}$.

The value of the petrophysical property at the percolation threshold, $V_{PT\text{-}SHL,}$ indicates a transition from unconnected to connected hydrocarbon flows. For V_{SHL} values below the percolation threshold, a connected path exists through these flow blocks resulting in recoverable effective permeabilities; for V_{SHL} values above the percolation threshold, a connected path does not exist through these flow blocks resulting in unrecoverable effective permeabilities. The same observations drawn from Figure 3 can be extended to the case of vertical effective permeability. Also, the petrophysical property V_{SHL} can be replaced with effective porosity ϕ_{EFF} to obtain the effective porosity percolation thresholds ϕ_{PT-EFF} for both horizontal and vertical flow.

Net sand cutoffs derived from percolation theory are well above the conventional cutoffs reported in the literature (Desbrandes). One of the possible reasons is that in log interpretation 100% volume fraction of shale indicates pure shale; however, values below 100% rock may also be non-net reservoir. In practice, the $V_{PT\text{-}SHL}$ cutoffs would be scaled by some average shale volume within non-reservoir rock.

Methodological Details

There are 5 steps in the proposed methodology for determining the $V_{PT\text{-}SHL}$ cutoff values:

I. Construct a lithofacies and petrophysical property model.

A sequential indicator simulation (SIS) program is used to construct binary facies models. All of the facies models are coded as 1's for sand or 0 for shale. Net porosity and permeability values of 0.40 and 1000mD, respectively, are assigned to all net lithologies; non-net porosity and permeability values of 0 and 0.001mD, respectively, are assigned to all non-net lithologies.

II. Apply a pressure gradient and calculate the steady-state flow rates and effective horizontal and vertical hydrocarbon permeabilities using a single phase flow simulation algorithm.

For each of the reservoir dependent parameters, the same pressure gradient is applied to the reservoir and the single phase steady-state flow rates are calculated within each flow block. Once the flow rates are calculated, the block effective permeabilities are easily calculated using Darcy's Law. Both the horizontal and vertical effective permeabilities are considered in this work. The horizontal permeability is taken as the geometric average of the effective Easting – X and Northing – Y permeabilities.

III. Observe the effective horizontal and vertical permeability versus V_{SHL} petrophysical property relationships via log-linear plots.

To visualize the relationship between the effective permeabilities and the petrophysical property variables, they are cross plotted on a log-linear scale similar to Figure 3.

IV. Fit the relationships generated in step III automatically with an appropriate model in order to determine the V_{PT-SHL} percolation threshold value.

One straightforward procedure for modeling effective permeability is the power model approach developed and tested by Deutsch, 1989. For this model, the effective permeability k_E is modeled as a power average of the component permeabilities:

$$k_E = \left[V_{SHL} k_{SHL}^{\omega} + \left(1 - V_{SHL}\right) k_{SS}^{\omega} \right]^{\frac{1}{\omega}}$$

where k_{SHL} and k_{SS} are the shale and sandstone permeabilities, respectively, and ω is some averaging power. The lower bound harmonic average corresponds to ω = -1, the geometric average corresponds to ω = 0 (with a limited expansion), and the upper bound arithmetic average corresponds to ω = 1.

An immediate limitation of modeling the effective permeability relationship seen in Figure 3 using this equation is the inflection point suggested by connecting the upper cloud flow blocks to the lower cloud flow blocks. To overcome this limitation, a piecewise version of Equation 1 is used to model the effective permeability above and below the percolation threshold:

$$k_E = \begin{cases} \left[V_{SHL} k_{SHL}^{\omega_A} + \left(1 - V_{SHL}\right) k_{SS}^{\omega_A} \right]^{\frac{1}{\omega_A}} & if\ V_{SHL} < V_{PT-SHL} \\ \hline \left[V_{SHL} k_{SHL}^{\omega_B} + \left(1 - V_{SHL}\right) k_{SS}^{\omega_B} \right]^{\frac{1}{\omega_B}} & if\ V_{SHL} < V_{PT-SHL} \end{cases}$$

where ω_A and ω_B are the ω values above and below the percolation threshold, respectively. A simulated annealing approach is considered within the framework of this piecewise model.

The first requirement for simulated annealing is an objective function, which is a measure of the difference between the desired result and a candidate result. The objective function is composed of one or more parameters to be perturbed, formally referred to as the optimization variables. For this work, the optimization variables are ω_A, ω_B and V_{PT-SHL}. The following constraints on these optimization variables must be honored:

$$ {}^{-}1 \le \left\{ \omega_A, \omega_B \right\} \le {}^{+}1 $$
$$ 0.0 \le V_{PT-SHL} \le 1.0 $$

The key feature of the simulated annealing method is to iteratively perturb the optimization variables, each time accepting or rejecting the perturbation according to a decision rule. The decision rule is based on whether or not the candidate result calculated using the perturbed parameters in the objective function is closer to the desired result or a maximum number of perturbations has been performed. In the context of this work, the objective function is to minimize the mean square error (MSE) between the calculated effective permeabilities from flow simulation and the ones calculated using the piecewise power law model:

$$MSE = \sum_{i=1}^{N} \left(k_{E_i} - k_{EF_i} \right)^2$$

where i = 1,…, N are the flow blocks in the model, k_E is the effective piecewise permeabilities and k_{EF} is the effective permeability from flow simulation.

The simulated annealing process progresses through the following steps: (1) establish an initial guess for ω_A, ω_B and $V_{PT\text{-}SHL}$ and calculate the initial value of the MSE (L_1 iteration), (2) randomly select a different set of ω_A, ω_B and $V_{PT\text{-}SHL}$ values and re-compute the MSE ($L_{N+1}{}^{th}$ iteration), (3) accept the new ω_A, ω_B and $V_{PT\text{-}SHL}$ values if the MSE decreases; reject them otherwise, (4) repeat steps 2 and 3 until a maximum number of iterations L_{MAX} is reached.

V. Apply the $V_{PT\text{-}SHL}$ percolation threshold values to logging measurements to determine net pay reservoir thickness.

Petrophysical well logs are the most abundant data source to quantify net pay in a petroleum reservoir. Hence, as they have the ability to measure mineralogy, porosity and mobility directly, they should be able to derive cutoff values precisely. There are many complicating factors involved in applying percolation threshold petrophysical properties to well logs. Dose, 2005 provides an excellent description of the available logging tools and methods.

Implementation and Interpretation

The dependencies investigated in this work are (1) global shale proportion, (2) spatial shale correlation, (3) net to non-net permeability contrast, (4) permeability distribution, (5) geological to flow block size contrast, and (6) depositional setting. Only the results for V_{SHL} are investigated; however, the methodology for other petrophysical properties is the same. Both horizontal and vertical flow $V_{PT\text{-}SHL}$ values are considered.

A set of base case reservoir and modeling parameters are frozen for each dependency. Tables 1 and 2 illustrate the base case parameters for the first five dependencies. There are two facies types: sand and shale. The proportion of sand and shale is 65% and 35%, respectively. The variogram model for sand and shale shares a 10% nugget effect and isotropic horizontal range of 120m. The vertical range for sand is 30m compared to 5m for shale. The net (sand) and non-net (shale) permeabilities are 1000 and 0.001mD, respectively. And there are 512 (8 x 8 x 8) geological blocks per flow simulation block within a field size of 320 x 320 x 32m. Tables 3 and 4 illustrate the parameters for the reservoir setting dependency. For the Mittelplate Dogger Delta and Cavendish settings, the net-to-gross ratio, channel thickness, width-to-thickness ratio, and sinuosity are reported. Here, there are 512 (8 x 8 x 8) geological blocks per flow simulation block within a field size of 1024 x 1024 x 32m. Finally, Table 5 shows the minimum, maximum, and initial ω_A, ω_B and $V_{PT\text{-}SHL}$ parameters used for the simulated annealing fit procedure.

Global Shale Proportion

The percolation threshold is determined for global shale proportions between 0.2 and 0.6 at an increment of 0.04. Figure 4 illustrates the PT results for 0.44 global shale proportion. Figure 5 shows the results for all 11 global shale proportion values from 20% to 60%. An increase in the global proportion of shale results in an increase in the PT values. To explain this, consider a low net and a high net reservoir with an identical correlation structure. If the same pressure gradient is applied to each, the pressure will "focus" on the fewer net streaks in the low net reservoir yielding a better sweep within the net, whereas the pressure will "spread out" in the high net reservoir. In practice, this means that higher shale proportions increase the importance of thin sand sections.

Correlation Structure

The second reservoir-specific dependency investigated is the spatial correlation structure of sand and shale lithofacies. The horizontal variogram range of 120m is changed from 5 m to 125m for a total of 25 shale correlation scenarios. Therefore, we investigate $a_{\mathrm{H}} : a_{\mathrm{V}}$ ratios from 1 to 25 by maintaining the 5m vertical range. Figure 6 shows the results for all 25 $a_{\mathrm{H}} : a_{\mathrm{V}}$ ratios. For horizontal flow, it is intuitive to see that an increase in the aerial continuity of shale and sand is related to higher $V_{PT\text{-}SH}$ values. This is similar to the first dependency when we observed increasing $V_{PT\text{-}SH}$ values for increasing shale proportion, that is, increasing $a_{\mathrm{H}} : a_{\mathrm{V}}$ ratios is similar to increasing the shale proportion in the horizontal direction. From Walter's Law, we can practically expect the same behavior in the vertical direction.

Permeability Contrast

The next dependency investigated is the contrast between net permeability and a constant non-net permeability $k_{\mathrm{NET}} : k_{\mathrm{N\text{-}NET}}$. The base case ratio is 10^6: 1 (= 1000/0.001). We investigate $k_{\mathrm{NET}} : k_{\mathrm{N\text{-}NET}}$ from $10^1 : 1$ to $10^6 : 1$ in factors of 10 for a total of 6 scenarios. For each scenario, the permeability contrast is modified by increasing the sand or net permeability by factors of 10. Figure 7 shows the results for all five $k_{\mathrm{NET}} : k_{\mathrm{N\text{-}NET}}$ ratios. A gradual decrease in the $V_{PT\text{-}SH}$ values for increasing $k_{\mathrm{NET}} : k_{\mathrm{N\text{-}NET}}$ ratios is observed. For the lower permeability contrasts, the conductivity of the reservoir is more homogenous and there is effectively less flow-restricting rock within the individual flow blocks. However, as the net permeability increases, the constant non-net permeability becomes a more severe restriction to flow. The result is a decreasing PT.

Modeling Scale

The next dependency investigated is not actually a property of the reservoir; nevertheless, it is a sensitive reservoir-specific variable in practice. The practitioner must decide on the relative size of the flow simulation block size to the small scale block size, and how to transfer cutoffs from one scale to the other. We define $S_{\mathrm{FLOW}} : S_{\mathrm{GEO}}$ as the ratio between the flow simulation block size to the small scale block size. We investigate $S_{\mathrm{FLOW}} : S_{\mathrm{GEO}}$ ratios of 2, 4, 8, 10, and 20, representing reduction factors of 8, 64, 512, 1000, and 80000, respectively. Figure 8 shows the results for all six $S_{\mathrm{FLOW}} : S_{\mathrm{GEO}}$ scenarios. For higher $S_{\mathrm{FLOW}} : S_{\mathrm{GEO}}$ ratios we observe an increase in the $\mathrm{V}_{\mathrm{PT\text{-}SH}}$ values. For higher $S_{\mathrm{FLOW}} : S_{\mathrm{GEO}}$ ratios, the geological model highly discretizes the flow blocks and there are many alternative paths hydrocarbon can take to span the flow block and form percolating clusters. Therefore, the volume of shale required to render high $S_{\mathrm{FLOW}} : S_{\mathrm{GEO}}$ blocks unconnected is high.

Channel Reservoir

We have considered only stochastic binary rocktype models. However, many geologic processes are better described by modeling discrete events, e.g., fluvial channels. This dependency considers the particular depositional setting. The parameters of the channel model are listed in Table 3. Figure 9 shows the percolation threshold results from one representative volume. We observe that virtually the entire reservoir is connected and net. The horizontal and vertical $V_{PT\text{-}SH}$ values are 0.96 and 0.91, respectively. Therefore, if there is any channel or levee material within a flow simulation block, it will almost always form a percolating cluster.

Discussion and Conclusion

The percolation threshold is the link between percolation theory and net pay determination. The resulting net pay criteria are tied to a net permeability that is supported by percolation theory. Percolation threshold petrophysical properties are suitable criteria for separating connected flow blocks from non-connected flow and are an explicit quantification of net pay criteria. Some practical considerations with respect to the application of logs in the light of percolation theory are given in Dose, 2005.

There is a large difference between conventional V_{SHL} cutoffs of 20 to 30% and the $V_{PT\text{-}SHL}$ cutoffs of 70 to 90% determined here. Time accounts for much of this discrepancy. Flow blocks deemed unconnected without the presence of a percolating cluster are surely non-recoverable; however connected flow blocks are not necessarily recoverable. That is, even though a particular flow block is deemed connected with a percolating cluster, the time for the hydrocarbon to flow through the block along the path of the percolating cluster may be too long to be practically recovered within a limited project life time. A dynamic flow simulation procedure could be implemented to incorporate a time dimension.

There are other relevant dependencies that would change the percolation threshold petrophysical property values such as the configuration of shale (structural, dispersed, laminated). Also, we can consider a combination of dependencies. However, the presented approach is restricted to the validity of Darcy's equation, which treats the rock as a continuum and does not separate between matrix and pore space.

The methodology for determining the net pay cutoff values is straightforward and can be applied to virtually any reservoir scenario. We have established some of the key relationships between net pay cutoffs and reservoir specific parameters so that an integrated approach to net pay determination can be undertaken.

References

Hearst, J., Nelson, P., and Paillett, F. *Well Logging for Physical Properties: A Handbook for Geophysicists, Geologists, and Engineers,* Second Edition. John Wiley & Sons, Ltd., England, 2000.

Etris, N. and Stewart, B. *Net-to-Gross Ratio.* Core Lab Reservoir Technologies Division, Calgary, Alberta, 2004.

Worthington, P. and Cosentino, L. *The Role of Cut-offs in Integrated Reservoir Studies.* SPE Paper 84387, 2003.

Deutsch, C. *Calculating Effective Absolute Permeability in Sandstone/Shale Sequences.* SPE Paper 17264, 1989.

Snyder, R. A *Review of the Concepts and Methodology of Determining “Net Pay”*. SPE Paper 3609, 1971.

Society of Petroleum Engineers and World Petroleum Congress. *Petroleum Reserve Definitions*. SPE, Richardson, Texas, 1997.

Jeffries, F. *Reservoir Volume Calculations with a Well Data System*. Transactions 8th Annual Logging Symposium, 1967.

Hunter, C., Kilgo, W., and Hickman, T. *The Development of a Marginal Clearfork Waterflood Prospect.* SPE Paper 20128, 1990.

Joshi, S. and Lahiri, G. Integrated Reservoir Characterization of Neelam Field. SPE Paper 39742, 1998.

Cobb, W. and Marek, F. Net Pay Determination for Primary and Waterflood Depletion Mechanisms. SPE Paper 48952, 1998.

Marquez, L., Gonzalez, M., Gamble, S., Gomez, E., Vivas, M., Bressler, H., Jones, L., Ali, S., and Forrest, G. Improved Reservoir Characterization of a Mature Field through an Integrated Multi-Disciplinary Approach: LL-04 Reservoir, Tia Juana Field, Venezuela. SPE Paper 71355, 2001.

Pirson, J. *Oil Reservoir Engineering*. McGraw Hill, New York, New York, 1958.

Stauffer, D. *Introduction to Percolation Theory.* Taylor and Francis London and Philadelphia, Frankfurt, Germany, 1985.

Sahimi, M. *Flow Phenomena in Rocks: From Continuum Models to Fractals, Percolation, Cellular Automata, and Simulated Annealing.* The American Physical Society, Reviews of Modern Physics, v. 65, No. 4, 1993.

Hammersley, J. and Welsh, D. *Percolation Theory and its Ramifications*. Contemporary Physics **21** No. 6., 1980.

Lenormand R. and Bories, S. Academic Science. B **291**, 1980.

Katz, A., and Thompson, A. *Quantitative Prediction of Permeability in Porous Rock*. Physical Review B, vol. 34, no. 11, 1986.

Kirkpatrick, S. *Percolation and Conduction*. Reviews of Modern Physics **45** No. 4., 1973.

Sykes, M. and Essam, J. *Exact Critical Percolation Probabilities for Site and Bond Problems in Two Dimensions*. Journal of Mathematical Physics **5**, 1964.

Mattox, C. and Dalton, R. *Reservoir Simulation,* Monograph Volume 13. SPE, Henry L. Doherty, Richardson, Texas, 1990.

Deutsch, C. *Geostatistical Reservoir Modeling*. Oxford University Press, 2002.

Deutsch, C. and Journel, A. *GSLIB: Geostatistical Software Library: and User’s Guide*, Oxford University Press, New York, 2nd Ed., 1998.

Dose, T., Strobel, J., and McLennan, J. *An Integrated Approach to Net Pay Determination*. DGMK Fruehjahrstagung., Fachbereich Aufsuchung und Gewinnung, Celle, Germany, 2005.

Lithology	Global Proportion (%)	Variogram Model	Permeability k (mD)
Sand	65.0	$\gamma(h) = 0.1 + 0.9 Sph(h)_{\substack{a_h=120 \\ a_v=30}}$	1000
Shale	35.0	$\gamma(h) = 0.1 + 0.9 Sph(h)_{\substack{a_h=120 \\ a_v=5}}$	0.001

Table 1: the reservoir-specific parameters of the base case model.

GEOLOGICAL GRID				FLOW SIMULATION GRID			
COORDINATE	NUMBER	MINIMUM	SIZE	COORDINATE	NUMBER	MINIMUM	SIZE
Easting - X	64	2.5	5	Easting - X	8	20	40
Northing - Y	64	2.5	5	Northing - Y	8	20	40
Elevation - Z	32	0.5	1	Elevation - Z	4	4	8
TOTAL BLOCKS	131,072			TOTAL BLOCKS	256		

Table 2: the modeling scale implemented for the base case models.

I. Dogger				
Geomoetry	Net : Gross	Channel Thickness (m)	Channel Width : Thickness	Sinuosity
	0.4	20	100	Medium
Lithology	Channel Fill	Channel Outline	Levee	Floodplain
Permeability (mD)	800	0.01	800	0.01

II. Cavendish				
Geomoetry	Net : Gross	Channel Thickness (m)	Channel Width : Thickness	Sinuosity
	0.2	20	100	Low
Lithology	Channel Fill	Channel Outline	Levee	Floodplain
Permeability (mD)	800	0.01	800	0.01

Table 3: the reservoir-specific parameters for the reservoir settings investigated.

GEOLOGICAL GRID				FLOW SIMULATION GRID			
COORDINATE	NUMBER	MINIMUM	SIZE	COORDINATE	NUMBER	MINIMUM	SIZE
Easting - X	64	8	16	Easting - X	8	20	40
Northing - Y	64	8	16	Northing - Y	8	20	40
Elevation - Z	32	0.078	0.156	Elevation - Z	4	4	8
TOTAL BLOCKS	131,072			TOTAL BLOCKS	256		

Table 4: the modeling scale implemented for the reservoir setting dependency.

SIMULATED ANNEALING			
PARAMETER	MINIMUM	MAXIMUM	INITIAL
ω_B	-1.0	1.0	0.50
ω_A	-1.0	1.0	-0.50
$V_{PT\text{-}SHL}$	0.0	1.0	0.69

Table 5: the simulated annealing parameters used for all dependency cases.

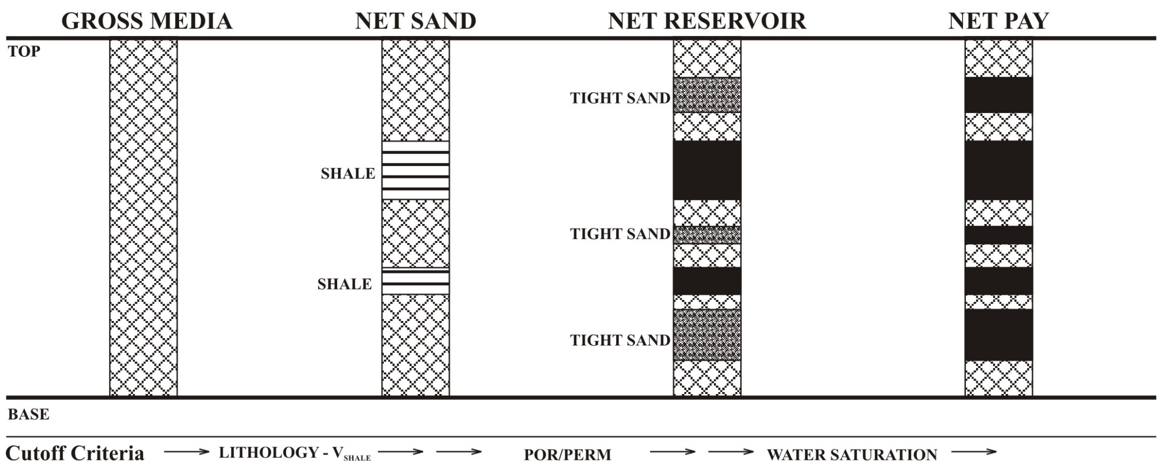

Figure 1: (Worthington, 2003) **-** Determination of net sand, net reservoir, and net pay according to lithology, porosity and permeability cutoffs, respectively.

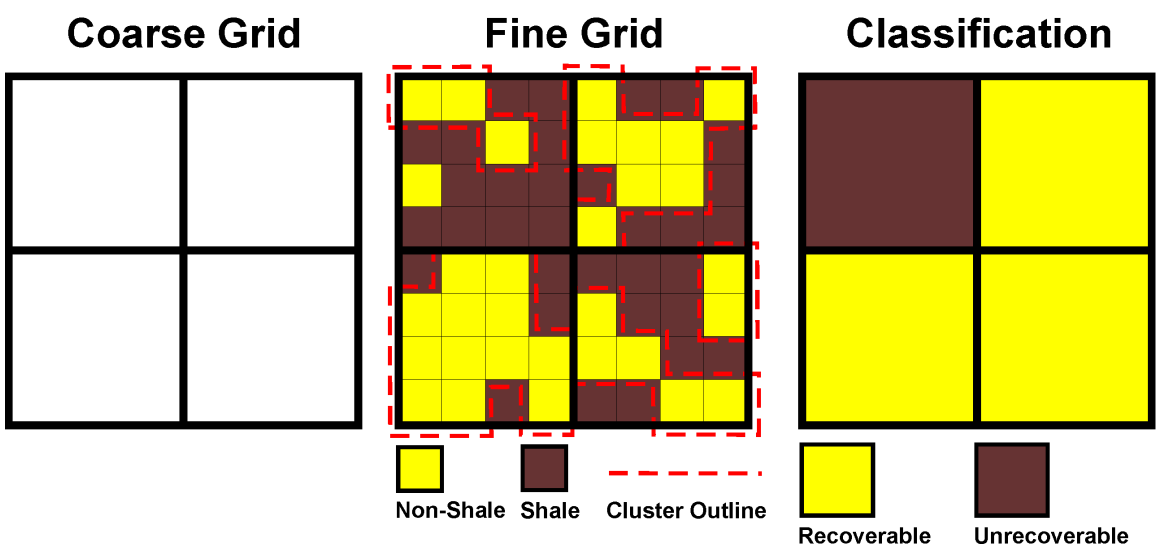

Figure 2: An illustration of correlated percolation. The pressure gradient is applied from left to right. Figure 2(a) shows a 2 x 2 array of flow simulation blocks. The 8 x 8 geological model shown in Figure 2(b) is subjected to a pressure gradient in order to calculate the effective absolute permeabilities of the flow blocks in (a). Figure 2(c) shows which blocks are commercially recoverable.

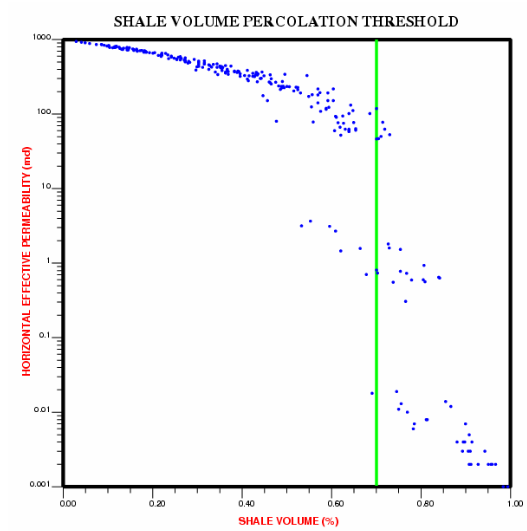

Figure 3: A plot of horizontal effective permeability versus V_{SHL}. The vertical line is drawn at the percolation threshold $V_{PT\text{-}SHL}$.

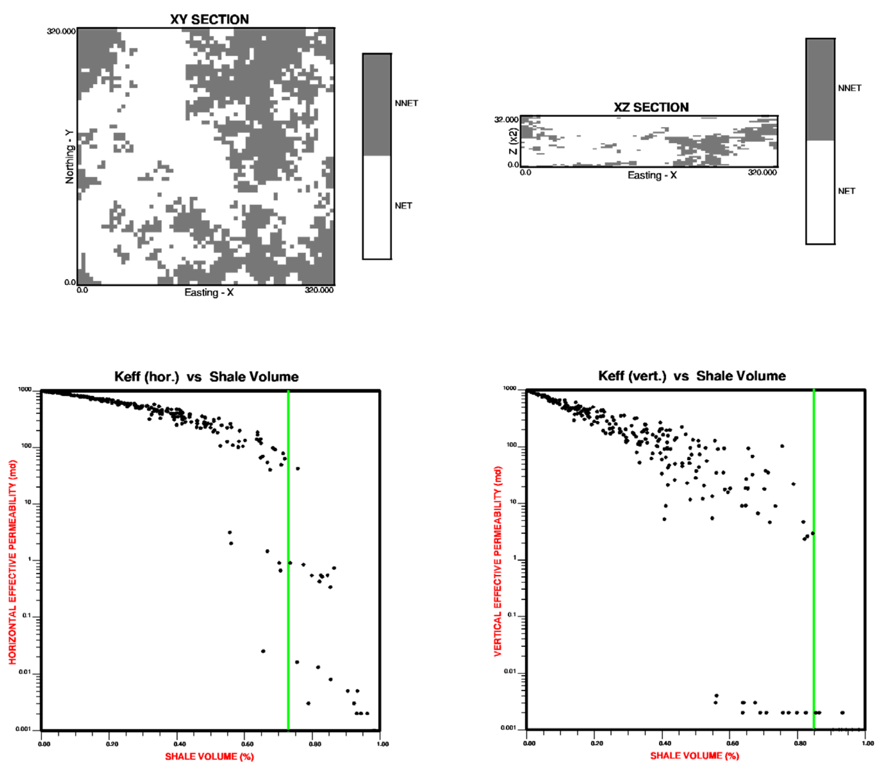

Figure 4: The heterogeneity models (top) and percolation results for 44% global shale proportion.

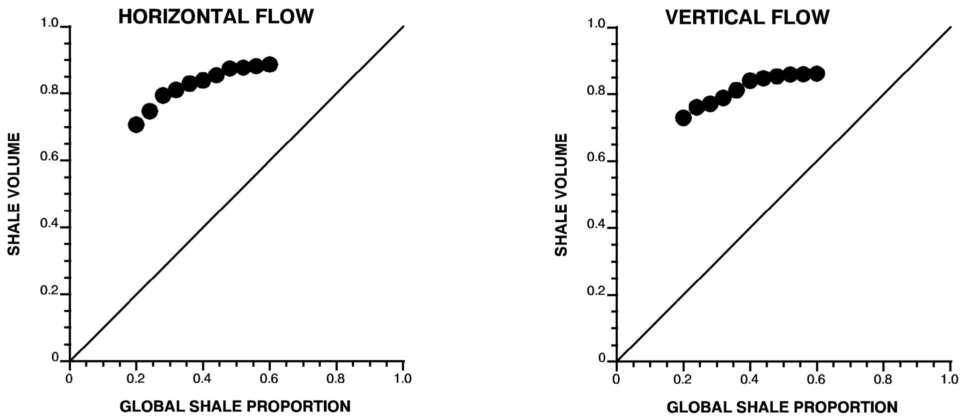

Figure 5: the percolation threshold results for the global shale proportion dependency.

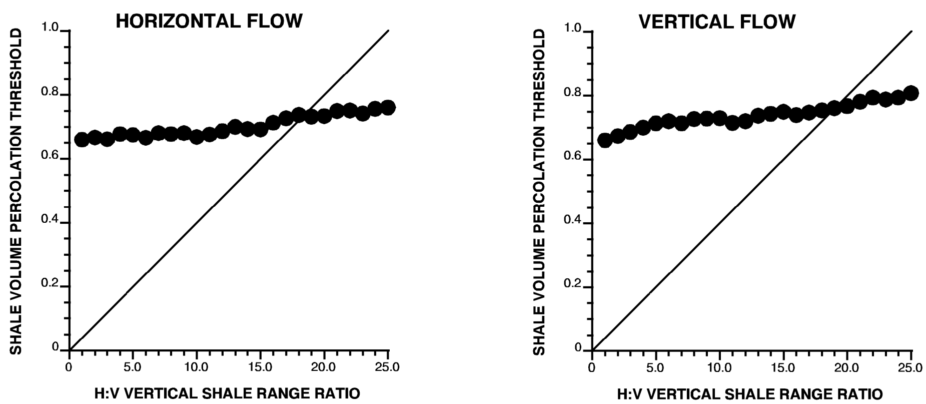

Figure 6: the percolation threshold results for the variogram range dependency.

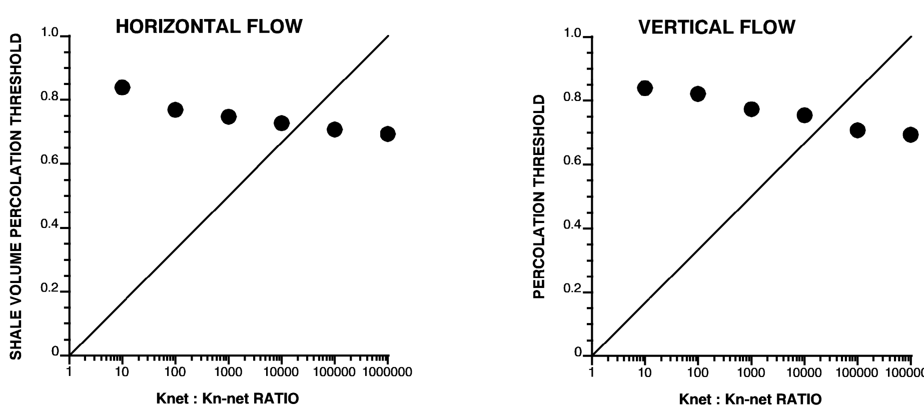

Figure 7: the percolation threshold results for the permeability contrast dependency.

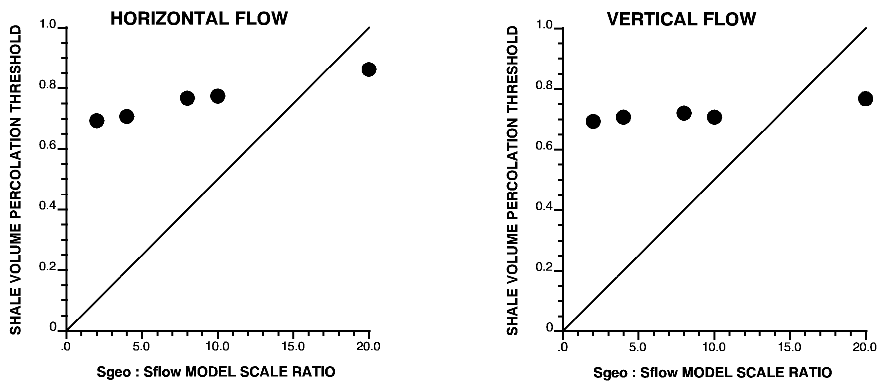

Figure 8: the percolation threshold results for the model scale dependency.

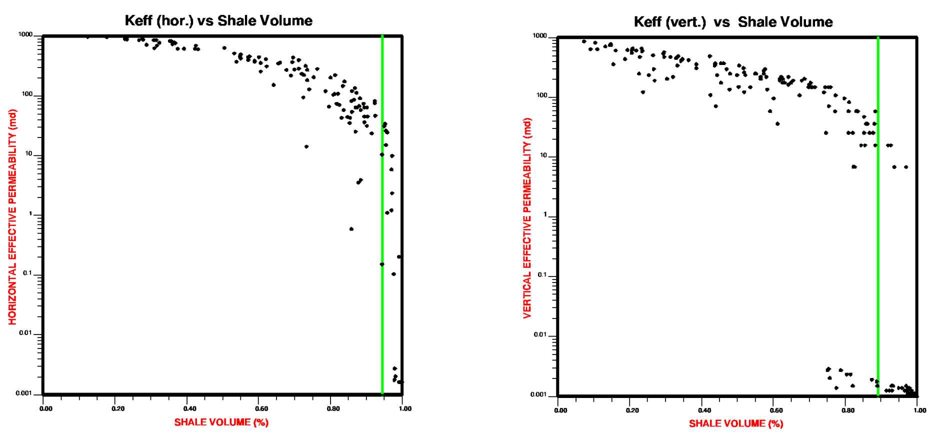

Figure 9: the percolation threshold results for the fluvial channel setting.